# Optical trapping through the localized surface-plasmon resonance of engineered gold nanoblock pairs

**Yoshito Tanaka and Keiji Sasaki***

*Research Institute for Electronic Science, Hokkaido University, Sapporo 001-0020, Japan*
**sasaki@es.hokudai.ac.jp*

**Abstract:** We have investigated the plasmonic trapping of dielectric nanoparticles by using engineered gold nanoblock pairs with ~5-nm gaps. Pairs with surface-plasmon resonance peaks at the incident wavelength allow the trapping of 350-nm-diameter nanoparticles with 200 W/cm$^2$ laser intensities, and their plasmon resonance properties and trapping performance are drastically modified by varying the nanoblock size of ~20%. In addition, plasmon resonance properties of nanoblock pairs strongly depend on the direction of the linear polarization of the incident laser, which determines the trapping performance.



**OCIS codes:** (250.5403) Plasmonics; (350.4855) Optical manipulation; (290.5870) Scattering, Rayleigh.

## References and links

1. K. Okamoto and S. Kawata, "Radiation force exerted on subwavelength particles near a nanoaperture," Phys. Rev. Lett. **83**(22), 4534–4537 (1999).
2. P. C. Chaumet, A. Rahmani, and M. Nieto-Vesperinas, "Optical trapping and manipulation of nano-objects with an apertureless probe," Phys. Rev. Lett. **88**(12), 123601 (2002).
3. L. Novotny, R. X. Bian, and X. S. Xie, "Theory of nanometric optical tweezers," Phys. Rev. Lett. **79**(4), 645–648 (1997).
4. M. L. Juan, R. Gordon, Y. Pang, F. Eftekhari, and R. Quidant, "Self-induced back-action optical trapping of dielectric nanoparticles," Nat. Phys. **5**(12), 915–919 (2009).
5. H. Xu and M. Käll, "Surface-plasmon-enhanced optical forces in silver nanoaggregates," Phys. Rev. Lett. **89**(24), 246802 (2002).
6. A. N. Grigorenko, N. W. Roberts, M. R. Dickinson, and Y. Zhang, "Nanometric optical tweezers based on nanostructured substrates," Nat. Photonics **2**(6), 365–370 (2008).
7. M. Righini, P. Ghenuche, S. Cherukulappurath, V. Myroshnychenko, F. J. García de Abajo, and R. Quidant, "Nano-optical trapping of Rayleigh particles and Escherichia coli bacteria with resonant optical antennas," Nano Lett. **9**(10), 3387–3391 (2009).
8. W. Zhang, L. Huang, C. Santschi, and O. J. F. Martin, "Trapping and sensing 10 nm metal nanoparticles using plasmonic dipole antennas," Nano Lett. **10**(3), 1006–1011 (2010).
9. Y. Tsuboi, T. Shoji, N. Kitamura, M. Takase, K. Murakoshi, Y. Mizumoto, and H. Ishihara, "Optical trapping of quantum dots based on gap-mode-excitation of localized surface plasmon," Phys. Chem. Lett. **1**(15), 2327–2333 (2010).
10. Y. Tanaka, H. Ishiguro, H. Fujiwara, Y. Yokota, K. Ueno, H. Misawa, and K. Sasaki, "Direct imaging of nanogap-mode plasmon-resonant fields," Opt. Express **19**(8), 7726–7733 (2011).
11. E. Hao and G. C. Schatz, "Electromagnetic fields around silver nanoparticles and dimers," J. Chem. Phys. **120**(1), 357–366 (2004).
12. M. Inoue and K. Ohtaka, "Surface enhanced Raman scattering by metal spheres. I. Cluster effect," J. Phys. Soc. Jpn. **52**(11), 3853–3864 (1983).
13. M. Righini, A. S. Zelenina, C. Girard, and R. Quidant, "Parallel and selective trapping in a patterned plasmonic landscape," Nat. Phys. **3**(7), 477–480 (2007).
14. L. Huang, S. J. Maerkl, and O. J. F. Martin, "Integration of plasmonic trapping in a microfluidic environment," Opt. Express **17**(8), 6018–6024 (2009).
15. U. Kreibig and M. Vollmer, *Optical Properties of Metal Clusters* (Springer, Berlin, 1995).
16. K. Ueno, V. Mizeikis, S. Juodkazis, K. Sasaki, and H. Misawa, "Optical properties of nanoengineered gold blocks," Opt. Lett. **30**(16), 2158–2160 (2005).
17. H. Fischer and O. J. F. Martin, "Engineering the optical response of plasmonic nanoantennas," Opt. Express **16**(12), 9144–9154 (2008).

#148513 - $15.00 USD Received 2 Jun 2011; revised 21 Jul 2011; accepted 19 Aug 2011; published 22 Aug 2011

18. Y. Tanaka, H. Yoshikawa, T. Itoh, and M. Ishikawa, "Surface enhanced Raman scattering from pseudoisocyanine on Ag nanoaggregates produced by optical trapping with a linearly polarized laser beam," J. Phys. Chem. C **113**(27), 11856–11860 (2009).
19. Y. Tanaka, H. Yoshikawa, T. Itoh, and M. Ishikawa, "Laser-induced self-assembly of silver nanoparticles via plasmonic interactions," Opt. Express **17**(21), 18760–18767 (2009).
20. O. L. Muskens, V. Giannini, J. A. Sánchez-Gil, and J. Gómez Rivas, "Optical scattering resonances of single and coupled dimer plasmonic nanoantennas," Opt. Express **15**(26), 17736–17746 (2007).
21. J. Yguerabide and E. E. Yguerabide, "Light-scattering submicroscopic particles as highly fluorescent analogs and their use as tracer labels in clinical and biological applications," Anal. Biochem. **262**(2), 137–156 (1998).
22. K. Ueno, S. Juodkazis, T. Shibuya, V. Mizeikis, Y. Yokota, and H. Misawa, "Nanoparticle-enhanced photopolymerization," J. Phys. Chem. C **113**(27), 11720–11724 (2009).
23. G. Baffou, R. Quidant, and C. Girard, "Thermoplasmonics modeling: a Green's function approach," Phys. Rev. B **82**(16), 165424 (2010).
24. Y. Tanaka, H. Yoshikawa, and H. Masuhara, "Two-photon fluorescence spectroscopy of individually trapped pseudoisocyanine J-aggregates in aqueous solution," J. Phys. Chem. B **110**(36), 17906–17911 (2006).
25. C. Hosokawa, H. Yoshikawa, and H. Masuhara, "Optical assembling dynamics of individual polymer nanospheres investigated by single-particle fluorescence detection," Phys. Rev. E Stat. Nonlin. Soft Matter Phys. **70**(6 Pt 1), 061410 (2004).

The optical trapping of nanometer-sized objects by using plasmonic nanostructures has attracted considerable attention in recent years because it significantly improves the trapping performance compared with conventional optical tweezers that use a tightly focused laser beam [1–9]. Localized surface plasmons, i.e., resonant charge-density oscillations confined to metal nanostructures, can efficiently convert propagating light into nanoscale confined and strongly enhanced optical fields, which generate high-intensity gradients responsible for the trapping mechanism. Among the huge variety of plasmonic nanostructures, a pair of metal nanoparticles separated by a nanometric gap produces an intense optical spot that is approximately two orders of magnitude smaller than the wavelength of the incident light [10–12], and it enables the optical trapping and confinement of dielectric nanoparticles such as polystyrene and living biological specimens with reduced laser intensity compared with conventional optical tweezers [6,7]. Furthermore, the nanogap structure was shown to trap metal and semiconductor nanoparticles with 10-nm dimensions [8,9]. The parallel trapping of micro- and nanoparticles has also demonstrated using patterned plasmonic nanostructures [7,13]. This plasmonic trapping by nanostructures deposited on a substrate is a promising technique for future biological and chemical lab-on-a-chip devices operated with light [14].

The localized surface plasmon also gives rise to spectrally selective light absorption and scattering. This plasmon resonance property strongly depends on the geometry and size of nanostructures. For example, anisotropic nanostructures such as nanorod and nanoparticle pairs have multiple resonance peaks [15–20]. Moreover, by varying the size of the gold and silver nanostructures, their color covers an extended wavelength range that includes most of the visible and infrared regions [15,21]. Thus, tailoring the structural geometry and size allows a direct control of the plasmon resonance property.

In this study, we demonstrate that the size and orientation of pairs of gold nanoblocks with ~5-nm determine their surface-plasmon resonance properties and trapping performance in conjunction with the wavelength and the polarization direction of the incident laser.

#148513 - $15.00 USD Received 2 Jun 2011; revised 21 Jul 2011; accepted 19 Aug 2011; published 22 Aug 2011

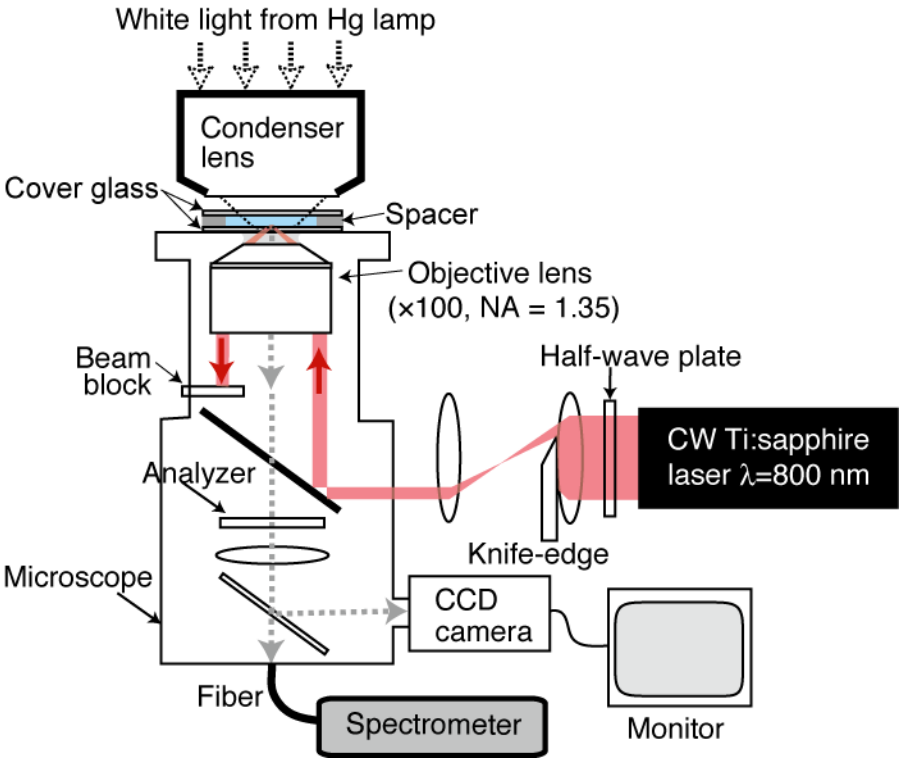


Fig. 1. Schematic of the experimental setup.

Figure 1 illustrates the optical setup. A continuous-wave Ti:sapphire laser (800-nm wavelength, 100-kHz linewidth) was used as the plasmonic-trapping light source. The linearly polarized beam was introduced into an inverted optical microscope and was focused by an oil-immersion objective [100 ×, numerical aperture (NA) = 1.35]. A section of the focused beam with the incident angle smaller than the critical angle was masked by a knife edge at the pupil plane of the imaging system, and thus, samples were illuminated under focused total internal reflection (TIR, spot area = 0.9 μm × 2.7 μm). The polarization angle of the incident beam was controlled by a half-wave plate. A 50-μm-deep liquid chamber containing 350-nm-diameter spherical polystyrene particles (refractive index of 1.57) in water (refractive index of 1.33) was prepared on a glass substrate with nanostructures. The particle concentration of 2.7 x $10^9$ particles/ml results in average numbers of 1.6 x $10^{-3}$ nanoparticles in the observation volume obtained from the spot area and decay distance (0.3 μm) of evanescent wave. The plasmonic trapping was viewed using a CCD camera to monitor scattered light from trapped particles by disturbing the evanescent field. Note that nanoparticles were not trapped using only the focused TIR irradiation without plasmonic nanostructures.

Surface-plasmon resonance properties of nanostructures were characterized by their extinction spectra. Collimated white light from a halogen lamp illuminated sample through a condenser lens. Transmitted white light through the sample was collected by the same microscope objective, passed through an optical fiber, and directed to an optical spectrometer equipped with a CCD detector cooled to −120 °C by liquid $N_2$. A ~0.5-μm-diameter collection area was used for the objective-fiber combination used here. Extinction spectra of the nanostructures were obtained by calculating $(I_b(\lambda)-I_m(\lambda))/I_b(\lambda)$, where $I_m(\lambda)$ and $I_b(\lambda)$ are the spectra of the transmitted white light through the sample with and without the nanostructures, respectively. An absorptive sheet polarizer was placed in front of the detector to analyze the polarization of transmitted white light.

#148513 - $15.00 USD Received 2 Jun 2011; revised 21 Jul 2011; accepted 19 Aug 2011; published 22 Aug 2011

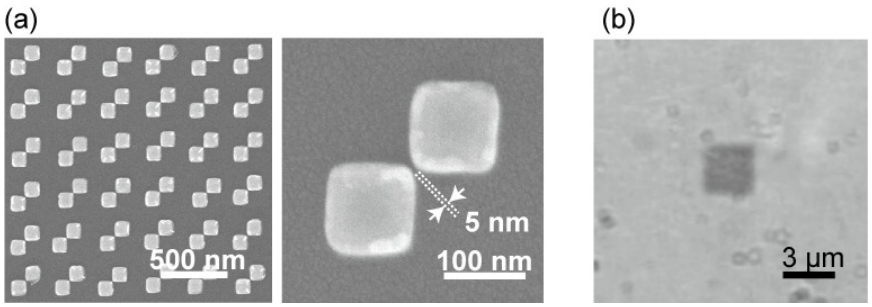


Fig. 2. (a) SEM and (b) transmitted images of an array of pairs of gold nanoblocks with 5-nm gaps. The right side of panel (a) shows a single nanoblock pair.

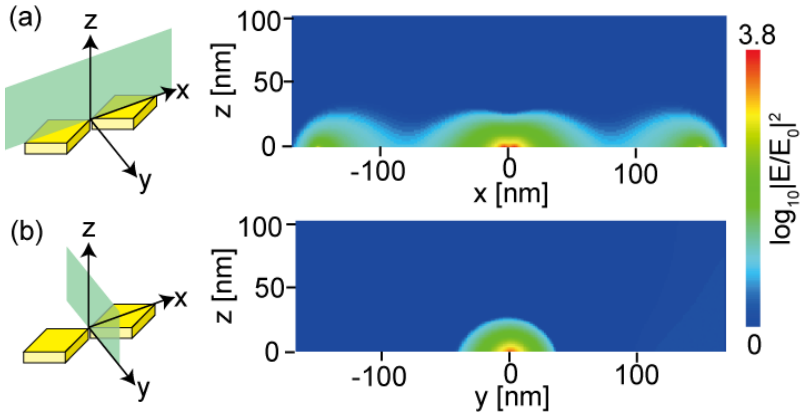


Fig. 3. Calculated near-field distributions near a model gold nanoblock pair at an 800-nm incident wavelength. Block size = 80 nm × 80 nm × 30 nm and gap distance = 5 nm. (a) *xz* plane and (b) *yz* plane on the pair as shown to the left side of panels (a) and (b), respectively.

A nanostructured sample is shown in the scanning electron microscope (SEM) image of Fig. 2(a). The sample was fabricated on a glass substrate by using electron beam lithography (EBL) and lift-off techniques [16,22]. Briefly put, the EBL technique was used to define masks of planar patterns of nanostructures on substrates and thin gold films were deposited over the mask by sputtering. Gold nanostructures were subsequently obtained by a lift-off of protected areas. This method yielded regular 3 μm × 3 μm two-dimensional arrays of pairs of diagonally aligned gold nanoblocks with nanometer-scale gaps. Within the array, all nanoblock pairs were oriented in the same direction.

Data discussed here were obtained from three samples with the same gap distance $d \approx 5$ nm, height $h = 40$ nm, and pair-pair separation $s = 320$ nm. However, in-plane sizes of nanoblocks differed. With such a small gap distance, the electromagnetic interaction between two nanoblocks splits the localized plasmon resonance of an individual nanoblock into two resonances of longitudinal and transverse modes for the nanoblock pair [15]. The excitation of the longitudinal mode leads to a large field enhancement around the gap between nanoblocks [10,22]. Note that this field enhancement extends not only within the nanogap but also outside it (see Fig. 3), which is important for the plasmonic trapping of nanoparticles larger than the gap size. Although it was difficult to observe an isolated pair of nanoblocks in the optical micrograph, the nanoblock array was clearly imaged, as shown in Fig. 2(b). In addition, because nanoparticles experience an optical force near the nanostructure surface, they could be trapped with a higher probability for a pair array, whose surface area is relatively large compared with a single pair. These features were convenient for our experiments.

#148513 - $15.00 USD Received 2 Jun 2011; revised 21 Jul 2011; accepted 19 Aug 2011; published 22 Aug 2011

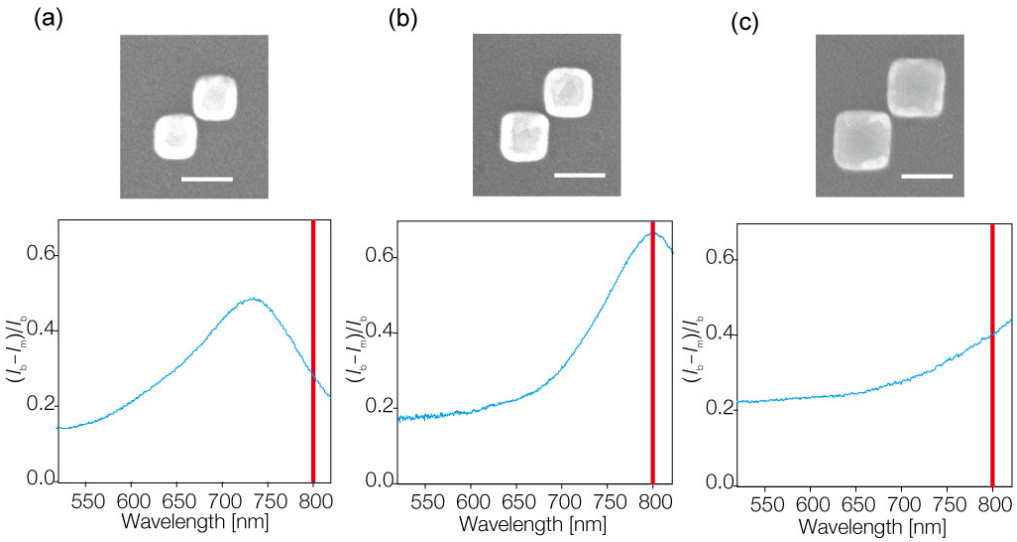


Fig. 4. SEM images of single gold nanoblock pairs with 5-nm gaps (top) and extinction spectra from arrays of the nanoblock pairs (longitudinal polarization) immersed in water (bottom). Nanoblock sizes: (a) 70 nm × 70 nm × 40 nm, (b) 80 nm × 80 nm × 40 nm, (c) 100 nm × 100 nm × 40 nm. Scale bar = 100 nm. The vertical red line in the spectra gives the incident laser wavelength.

Figure 4 (top) shows three single nanoblock pairs of size 70 nm × 70 nm × 40 nm, 80 nm × 80 nm × 40 nm, and 100 nm × 100 nm × 40 nm. Longitudinal plasmon resonance peaks of these pairs are clearly different from each other (see Fig. 4, bottom). The pairs with an 80-nm block width exhibit a surface-plasmon resonance peak at an 800-nm incident wavelength, and the 70- and 100-nm pairs exhibit surface-plasmon resonance peaks below and above 800 nm, respectively. The extinction intensity at 800-nm for the 80-nm pairs is 2.4 and 1.7 times higher than those for the 70- and 100-nm pairs, respectively. The calculated field enhancement factor at 800-nm ($M_{800} = |E_{max}/E_0|^2$) is about 6300 for the 80-nm pairs (see Fig. 3), and the field enhancement factors ($M_{800}$) for the 70- and 100-nm pairs are 2.3 and 2.0 times lower, respectively. Such nanoblock pairs of different sizes are used to optically trap nanoparticles. The incident laser power was fixed at 15 μW, corresponding to intensity in the spot area of 750 W/cm$^2$. For conventional optical tweezers, which were obtained by removing the knife edge and beam block (see Fig. 1), an intensity of 2 MW/cm$^2$ was required to trap 350-nm-diameter polystyrene particles for a period of a few tens of seconds. This intensity is more than three orders of magnitude larger than that required for the plasmonic trapping of the same particles. Other groups report the plasmonic trapping of 200-nm-diameter polystyrene particles with the incident intensity > kW/cm$^2$ [7]. In addition to optical gradients, coupling to the surface plasmon resonances can produce local heating in the metal and heat dissipation within the chamber, which results in convection. However, a local temperature elevation in the gold nanostructure for low incident intensity of 750 W/cm$^2$ is estimated to be less than 0.1 °C from some previous reports which experimentally and theoretically evaluate it [9,23]. Thus, the trapping contribution from plasmon-thermal fluid convection can be negligible.

#148513 - $15.00 USD Received 2 Jun 2011; revised 21 Jul 2011; accepted 19 Aug 2011; published 22 Aug 2011

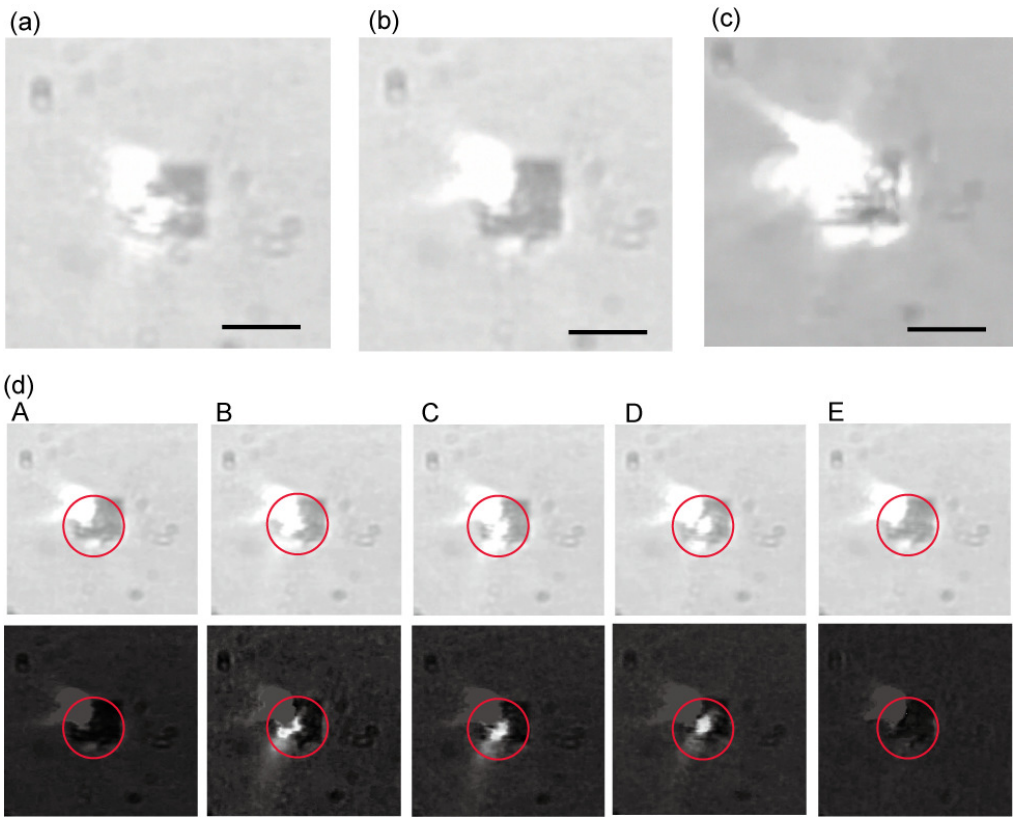


Fig. 5. Optical plasmonic trapping of 350-nm polystyrene particles with nanoblock pairs at the incident laser power of 15-μW. Block sizes: (a) (Media 1) 70 nm × 70 nm × 40 nm, (b) (Media 2) 80 nm × 80 nm × 40 nm, (c) (Media 3) 100 nm × 100 nm × 40 nm. Scale bar = 3 μm. (d) Top: Snapshots taken from (b) (Media 2) at several times: (A) 0.5 s, (B) 1.0 s, (C) 6.0 s, (D) 14.0 s, and (E) 15.0 s. Bottom: Images obtained by subtracting the first frame of the movie from each snapshot. The plasmonic trapping takes place in the red cycles of (d). Bright scattered light is observed around pairs. When nanoparticles pass sufficiently close to pairs, they get trapped and appear as bright scattering centers.

Figure 5 (a)-(c) (Media 1, Media 2, Media 3) show plasmonic trapping of 350-nm particles. In the first frame of these movies (see Fig. 5 (a)-(c)), the particles are not trapped and bright scattered light is observed around nanoblock pairs. When nanoparticles pass sufficiently close to the pairs, they get trapped and appear as bright scattering spots, as shown in Fig. 5 (d). The position of this bright spots fluctuates slightly, suggesting that particle Brownian motion is still present. This phenomenon distinguishes between light scattering from particles and that from nanoblock pairs. The escape of particles from the pairs is known from the disappearance of the fluctuating bright spots. On such process, the increase and decrease of the light scattered from particles are done in one step. On the other hand, the scattered light must gradually increase and decrease for optical trapping of multiple particles, as proved in the previous study [24,25]. In addition, as aforementioned, the average number of nanoparticles in the observation volume is estimated to be $1.6 \times 10^{-3}$ particles. These strongly support single-particle trapping in the present experiments. For the 70- and 100-nm nanoblock widths, nanoparticles become trapped and then escape from pairs within a few seconds, as shown in Figs. 5(a) (Media 1) and 5(c) (Media 3), respectively. However, the 80-nm nanoblock pairs optically traps nanoparticles for at least ten times longer, as shown in Fig. 5(b) (Media 2). Thus, we conclude that nanoblock pairs with the plasmon resonance peak at the incident wavelength allow the stable trapping of nanoparticles. Note that a variation in the

#148513 - $15.00 USD Received 2 Jun 2011; revised 21 Jul 2011; accepted 19 Aug 2011; published 22 Aug 2011

block size of only 20% drastically modifies the plasmon resonance property and the trapping performance of nanoblock pairs.

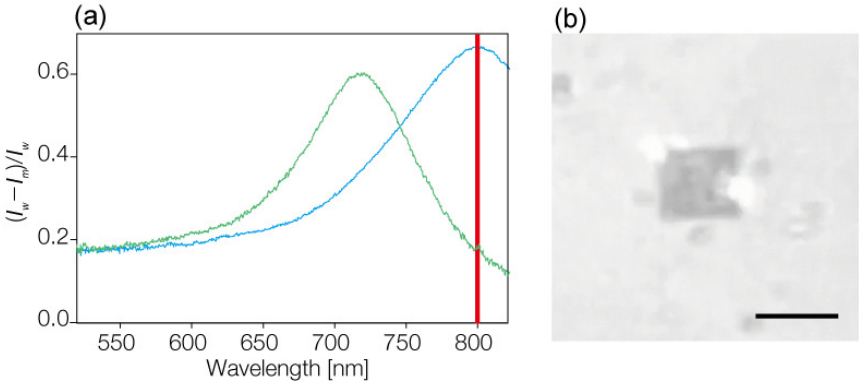


Fig. 6. (a) Extinction spectra of pairs of nanoblocks of 80 nm × 80 nm × 40 nm in size with longitudinal (blue) and transverse (red) polarizations. (b) (Media 4) Plasmonic trapping of a 350-nm nanoparticle at a 4-μW incident power when the incident polarization is converted from longitudinal to transverse. Scale bar = 3 μm.

For 80-nm nanoblock pairs, the peak of the transverse plasmon resonance is away from the wavelength of the incident laser [Fig. 6(a)]. Moreover, nanogap-mode plasmons are not excited with transverse polarization, as shown in Refs [15,22]. Therefore, the trapping performance of nanoblock pairs changes when the incident polarization is converted from longitudinal to transverse. As shown in Fig. 6(b) (Media 4), this polarization conversion leads to a decrease in the light-scattering intensity from pairs and the subsequent release of trapped nanoparticles. The incident intensity of 200 W/cm$^2$ was four orders of magnitude less than that for conventional optical tweezers. With transverse polarization, we were unable to trap nanoparticles on pairs despite attempting to do so for five hours. Thus, for example, for two types of nanoblock pairs with longitudinal axes orthogonal to each other, we can select the trapping pair via the polarization of the incident laser.

In summary, we have investigated the trapping performance and the surface-plasmon resonance property of engineered pairs of gold nanoblocks with ~5-nm gaps. Pairs with surface-plasmon resonance peaks at the incident wavelength allow the plasmonic trapping of 350-nm-sized nanoparticles with a laser intensity four orders of magnitude smaller than conventional optical tweezers. The trapping performance and plasmon resonance property are drastically modified by varying the block size. In addition, the plasmon resonance property of nanoblock pairs strongly depends on the direction of the incident linear polarization, which determines the trapping performance of pairs. Thus, an arrangement of nanoblock pairs with various sizes and orientations can allow selective nanoparticle trapping and patterning that can be optically controlled by the incident optical wavelength and polarization. This technique offers a new potential for plasmonic trapping by metal nanostructures.

**Acknowledgments**

The authors would like to thank Profs. H. Misawa and K. Ueno of Hokkaido University for their help on fabrication of the metal structures. The present work was partly supported by the Ministry of Education, Culture, Sports, Science and Technology of Japan by the KAKENHI Grant-in-Aid for Scientific Research on the Priority Area “Strong Photon-Molecule Coupling Fields” (No. 470, 1904900209) and the Young Scientists (B) (2171009009) grant to Yoshito Tanaka.

#148513 - $15.00 USD Received 2 Jun 2011; revised 21 Jul 2011; accepted 19 Aug 2011; published 22 Aug 2011